Missouri University of Science and Technology
Scholars' Mine

Physics Faculty Research & Creative Works | Physics

01 Sep 1979

Doubly Differential Cross Sections for Proton-Impact Ionization of Argon

Don H. Madison
Missouri University of Science and Technology, madison@mst.edu

Steven Trent Manson

Follow this and additional works at: https://scholarsmine.mst.edu/phys_facwork

 Part of the Physics Commons

Recommended Citation

D. H. Madison and S. T. Manson, "Doubly Differential Cross Sections for Proton-Impact Ionization of Argon," *Physical Review A - Atomic, Molecular, and Optical Physics*, vol. 20, no. 3, pp. 825-833, American Physical Society (APS), Sep 1979.
The definitive version is available at https://doi.org/10.1103/PhysRevA.20.825

This Article - Journal is brought to you for free and open access by Scholars' Mine. It has been accepted for inclusion in Physics Faculty Research & Creative Works by an authorized administrator of Scholars' Mine. This work is protected by U. S. Copyright Law. Unauthorized use including reproduction for redistribution requires the permission of the copyright holder. For more information, please contact scholarsmine@mst.edu.

PHYSICAL REVIEW A VOLUME 20, NUMBER 3 SEPTEMBER 1979

Doubly differential cross sections for proton-impact ionization of argon

D. H. Madison
Department of Physics, Drake University, Des Moines, Iowa 50311

S. T. Manson
Department of Physics, Georgia State University, Atlanta, Georgia 30303
(Received 22 January 1979)

Proton-impact-ionization cross sections for argon which are differential in the energy and angle of the ejected electron have been calculated within the framework of the Born approximation using both Hartree-Slater and Hartree-Fock wave functions for the ejected electron. Results of the two types of calculations are compared with each other and with experiment. Differential cross sections for all five sub shells of argon are examined and particular attention is given to some interesting features of the K-shell cross sections. The range of applicability of the theoretical models is discussed.

I. INTRODUCTION

The problem of proton-impact ionization of atoms has been receiving considerable attention in the literature recently. Extensive experimental and theoretical work has been concentrated on obtaining total energy-dependent cross sections, particularly for the K and L shells of atoms.[1,2] In these works, it has been found that reasonable agreement between experiment and theory for total cross sections can be obtained using first-order classical, semiclassical, or quantum-mechanical perturbation theory with elementary wave functions describing the atomic charge distribution. Comparison of total cross sections with theoretical calculations does not represent an adequate test of theory, however, since important phenomena can be obscured or lost in the summing and averaging necessary for obtaining total cross sections. Comparing cross sections that are differential in one or more of the kinematic parameters represents a far better test.

A limited amount of double differential cross section (DDCS) work on atoms (differential in the energy and angle of the ionized electron) has appeared in the literature over the last few years. Most of this work has concentrated on proton-impact ionization of helium.[3-7] Helium is well suited for an initial study since it is known that the ionized electron has been ejected from a K shell. In these studies, it has been seen that semiclassical calculations are in poor agreement with the large-angle experimental data. On the other hand, the plane-wave Born approximation (PWBA) gives reasonable agreement with the DDCS data given even down to incident proton energies as low as 5 keV (Ref. 7) if the bound and continuum wave functions for the ionized electron are calculated as eigenfunctions of a realistic atomic potential. The largest difference between experiment and the PWBA is seen at small angles when the outgoing proton and electron have comparable velocities and charge exchange to the continuum[8] (CEC) becomes significant.

More recently, experimental proton-ionization work has appeared for ionization of atoms more complex than helium with a considerable interest in ionization of argon.[9-13] In these DDCS measurements, no discrimination is made between the different atomic subshells. As a result, these cross sections represent sums of DDCS for each of the five subshells of argon. From a theoretical point of view, examination of this problem is important for several reasons. (i) The outermost subshell (which dominates the cross section) is a $3p$ which has more structure and extent than a simple $1s$ shell. (ii) The PWBA has not been thoroughly tested for complex charge distributions. (iii) Photoionization results indicate a strong sensitivity of the $3p \rightarrow \epsilon d$ channel on the details of the atomic wave functions used.[14,15] This sensitivity will be important for charged particle scattering. (iv) The effect of CEC has not been scrutinized for complex atoms.

In this paper we have examined the proton-impact ionization of argon within the framework of the PWBA. Calculations were performed using Hartree-Slater (HS) wave functions for all discrete and continuum wave functions. In addition, calculations for the $3p \rightarrow \epsilon d$ channel were also performed using full Hartree-Fock (HF) wave functions for the discrete and final states. Some details of the calculation, as well as a very brief outline of the theoretical formulation are given in Sec. II; the details of the theory and method of calculation are given in Refs. 5 and 6.

The primary differences between the HS and HF calculations occur for ejected-electron energies less than 50 eV. In Sec. III, the results of our HS calculation for ejected-electron energies greater

 © 1979 The American Physical Society

than 50 eV are presented and compared with experimental results for argon. Section IV compares the HS results with the improved calculation which includes $3p \rightarrow \epsilon d$ in the HF approximation and an assessment is made of the limitations of the improvement. In Sec. V, the contribution of each shell of argon to the sum over shells is examined. Section VI examines some interesting properties of the DDCS for K-shell ionization and Sec. VIII contains the conclusions.

THEORY AND METHOD OF CALCULATION

In the PWBA, the basic ingredients of the cross sections are the matrix elements of the spherical Bessel functions, j_λ, between initial discrete wave functions U_{nl_0}/r and final continuum wave functions $U_{\epsilon l}/r$

$$R^{\lambda}_{nl_0,\epsilon l}(K) \equiv \int_0^\infty U_{\epsilon l}(r)^* j_\lambda(Kr) U_{nl_0}(r)\, dr\,. \tag{1}$$

Here Ka_0 is the momentum transfer (a_0 is the Bohr radius) and ϵ is the ejected-electron energy. In terms of these matrix elements and the phase shifts $\xi_l(\epsilon)$ of the various continuum waves, the triple differential cross sections (TDCS) can be written, i.e., the cross-section differential in the energy of the ejected electron, the angle of ejection, and the scattering angle of the proton. Since there is not data on the TDCS for proton-impact ionization, we consider the DDCS, i.e., energy and angular distribution of secondary electrons, which can be obtained by integrating the TDCS over the scattering angles of the proton to yield[5,6]

$$\begin{aligned}\frac{\partial^2\sigma_{nl_0,\epsilon k}}{\partial(\epsilon/R)d\Omega_e} = {} & \frac{2z^2a_0^2}{T/R}\,\frac{M}{m}N_{nl_0}\sum_{\substack{l,l'\\ \lambda,\lambda'\\ L}} i^{\lambda+\lambda'+l+l'} \\ & \times \exp[i(\xi_l-\xi_{l'})](2L+1)(2l+1)(2l'+1)(2\lambda+1)(2\lambda'+1) \\ & \times \begin{pmatrix} l' & \lambda' & l_0\\ 0 & 0 & 0\end{pmatrix}\begin{pmatrix} l & \lambda & l_0\\ 0 & 0 & 0\end{pmatrix}\begin{pmatrix} l & l' & L\\ 0 & 0 & 0\end{pmatrix}\begin{pmatrix} \lambda & \lambda' & L\\ 0 & 0 & 0\end{pmatrix}\begin{Bmatrix} \lambda & \lambda' & L\\ l & l' & l_0\end{Bmatrix} \\ & \times\left(\int_{K_{\min}}^{K_{\max}} P_L(\cos\theta_K)R^{\lambda}_{nl_0,\epsilon l'}(K)R^{\lambda}_{nl_0,\epsilon l}(K)\frac{d(Ka_0)}{(Ka_0)^3}\right)P_L(\cos\theta_e)\,,\end{aligned} \tag{2}$$

with N_{nl_0} the initial-state occupation number, θ_K the angle the momentum transfer makes with the proton beam, θ_e the angle of observation of the ejected electron, M and m are the proton and electron masses, respectively, T the incident proton energy, R the Rydberg energy (13.605 eV), and $\begin{pmatrix} a & b & c\\ d & e & f\end{pmatrix}$ and $\begin{Bmatrix} a & b & c\\ d & e & f\end{Bmatrix}$ the Wigner 3-j and 6-j symbols, respectively.

The one-particle wave functions were taken as solutions to the radial Schrödinger equation

$$\left(\frac{d^2}{dr^2}+E-V(r)-\frac{l(l+1)}{r^2}\right)U(r)=0 \tag{3}$$

with $V(r)$ the Hartree-Slater potential for the ground state of the atom as tabulated by Herman and Skillman.[16] For discrete states $E=\epsilon_{nl}$, the one-electron energy, and for continuum states, $E=\epsilon$, the kinetic energy of the ejected electron. In general small changes in the potential will result in small changes in the wave functions and, thus, in the subsequent matrix elements. In certain cases, this will not be true. To explore this, we look at the effective potential, $V_{\text{eff}}(r)=V(r)+l(l+1)/r^2$. The effective potentials for argon are given in Fig. 1 for $l=0$, 1, 2 and 3. From this figure, it is seen that V_{eff} for $l=2$ behaves qualitatively differentialy from the others: it has a barrier with attractive wells on either side. This barrier is the result of the balance between the attractive electrostatic and repulsive centrifugal potentials.[17] The addition of two large numbers of opposite sign yields a very small result (the sum is ~5% of each of the terms individually). Thus a small change in the electrostatic potential $V(r)$ can change the effective potential dramatically. Thus we have an *ab initio* criterion for when a more accurate calculation must be done. Since the barrier does not appear for the other partial waves, we are fairly safe in using HS functions in those cases.

To provide more accurate results, therefore, we have calculated the $3p \rightarrow \epsilon d$ matrix elements using HF wave functions for initial $3p$ and final ϵd states with full allowance for core relaxation. The details of this calculation are given elsewhere[14] where it was seen that, in photoionization, going

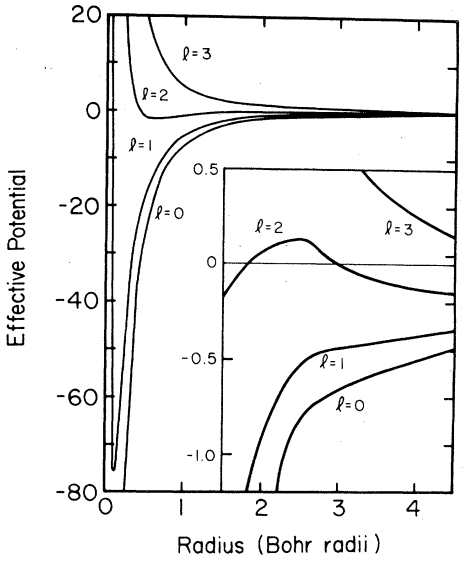

FIG. 1. Effective potential for argon in Ry (13.6 eV) for the first four partial waves.

from HS to HF reduced discrepancies between theory and experiment from a factor of 2 to about 20%.

III. HARTREE-SLATER CALCULATION

In Sec. IV, it will be shown that the differences between the HS and HF calculations are significant only for ejected-electron energies less than about 50 eV. In this section, we will compare the results of the HS calculation with experimental data for ejected-electron energies greater than 50 eV. We have performed the HS calculations for ejected-electron energies between 10 and 300 eV and incident proton energies between 5 keV and 5 MeV for ionization of all five subshells of argon. Complete tables of the differential cross sections for the shells or sum over shells can be obtained from one of the authors (D.H.M.).

The experiments which have been performed to date do not distinguish the subshells from which the electron has been ejected. As a result, the experimental differential cross sections represent cross sections summed over all the shells of the atom. In Fig. 2, the summed differential cross sections are compared with the experimental data of Crooks and Rudd,[9] Gabler *et al.*[10] and Criswell *et al.*[13] for 75-eV ejected electrons and incident proton energies between 50 keV and 5 MeV. As may be seen from the figure, the overall agreement between theory and experiment is reasonable over the entire angular range for the ejected electron except for small angles at 100 and perhaps 500 keV. This disagreement is readily understood

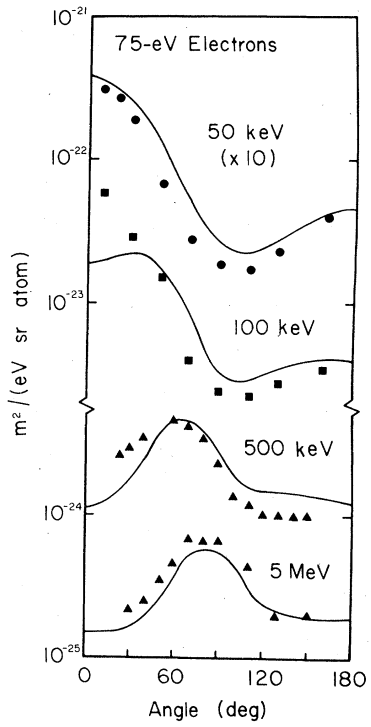

FIG. 2. DDCS for proton-impact ionization of argon. The results are presented for ejection of a 75-eV electron as a function of ejected-electron observation angle for incident protons with energies between 50 keV and 5 MeV. The solid curves are theoretical HS calculations. The experimental data are as follows: ● Criswell *et al.* (Ref. 13), ■ Crooks and Rudd (Ref. 9), and ▲ Gabler *et al.* (Ref. 10).

in terms of CEC.[8] The effect of CEC is known to be most important at small scattering angles when the velocity of the ejected electron matches the velocity of the proton. For a 75-eV electron, this velocity match would occur for a proton of about 150 keV. In this proton energy region, the experimental data should exhibit an enhanced cross section due to the charge exchange process over the theoretical calculation which does not include this effect. Figure 2 exhibits this behavior. The CEC effects are greatly reduced for 500-keV protons and are not apparent for 50-keV and 5-MeV protons. It is also interesting to note the good agreement between experiment and theory for 50-keV incident protons. It is surprising that the Born approximation is reliable at these low energies since this is the region where one might expect a molecular-orbital approach to be more appropriate. A similar surprising good agreement between experiment and theory for proton energies as low as 5 keV has been noted by Rudd and Madison[7] for ionization of helium.

Figure 3 shows a similar comparison for ejected

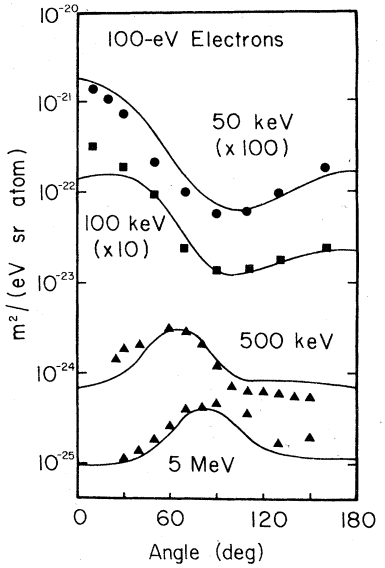

FIG. 3. Same as Fig. 2 except for 100-eV ejected electrons.

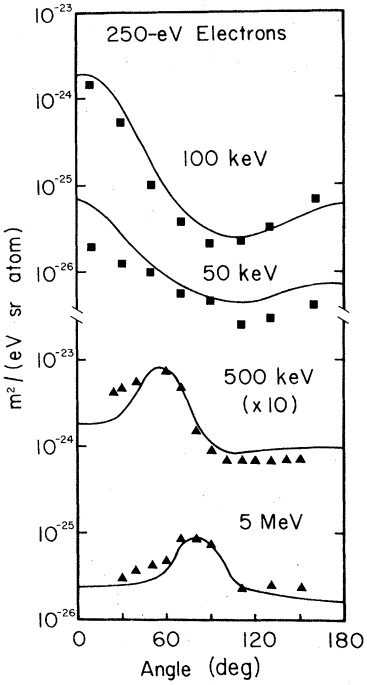

FIG. 4. Same as Fig. 2 except for 250-eV ejected electrons.

electrons with an energy of 100 eV. Examination of this figure yields conclusions similar to those obtained from Fig. 2. CEC would be most pronounced for 200-keV incident protons. Residual effects of this phenomena are observables at 100 and 500 keV, but again have disappeared by 50 keV and 5 MeV. The overall agreement between experiment and theory is quite good.

The final comparison between the HS calculation and experiment is presented in Fig. 4 for 250-eV ejected electrons. For 250-eV ejected electrons, the CEC effect at 500 keV is less pronounced than that observed for the lower ejected-electron energies. Comparison of the results of Fig. 4 with the two previous figures reveals two major differences. The first difference lies in the fact that the 50-keV experimental data is in worse agreement with the theoretical calculation. The significance of this disagreement is not clear since these cross sections are small and harder to measure experimentally.

The second difference lies in the behavior of the cross sections as a function of proton energy. It is interesting to note that for the lower electron energies, the cross sections generally tended to decrease with increasing proton energy, while for the 250-eV ejected electrons, the cross sections increase between 50 and 500 keV and then decrease. The phenomena observed here can be understood in terms of the proton-energy-dependent cross section for a fixed electron energy. This cross section rises to a maximum with increasing proton energy and then falls off. The peak in this function is around 50 keV for the lower ejected-electron energies, and the peak moves to higher proton energies with increasing ejected-electron energies. The proton-energy-dependent cross section has been examined by Criswell *et al.*[13]

IV. HARTREE-FOCK CALCULATIONS

If comparisons between the HS calculation of Sec. III and experiment are made for lower ejected-electron energies, significant deviations are seen. These differences between experiment and theory can be observed even for scattering angles greater than 90° and consequently cannot be attributed to CEC. As a result, it must be concluded that there is a deficiency in either the HS calculation or the original perturbation theory on which the calculation is based. In this section, we shall examine an improvement to the HS calculation.

A suggestion for improving the calculation comes from optical (photoionization) work on argon where it was found that the $3p \rightarrow \epsilon d$ channel has a Cooper minimum,[18,19] i.e., an energy at which the positive and negative contributions to the dipole matrix element just cancel. Calculations of Ar $3p$ photoionization show that HS wave functions predict a photoionization cross section that is too large at threshold by a factor of 2 and then drops much too rapidly to a Cooper minimum.[19,20] This deficiency

can be partially corrected by using HF wave functions for both initial discrete and final continuum states,[20] which reduces discrepancies in the photoionization cross section to about 20% and moves the theoretical Cooper minimum closer to the experimental one.

It will be shown in Sec. V, that for low ejected-electron energies, the outer shell dominates the ejected-electron spectrum. Further it is known that for Ar, as well as Kr and Xe, the $3p \rightarrow \epsilon d$ channel is dominant and the ejected-electron spectrum closely resembles the photoionization cross section.[21] This is a general phenomenon and it has been shown that for high enough incident proton energy, the low-energy electron spectrum is directly related to the photoionization cross section irrespective of the target atom (or molecule).[22,23]

For the above reasons, we have performed the DDCS calculation using a HF formalism for $3p \rightarrow \epsilon d$ and the HS approximation for the rest of the calculation, as discussed in Sec. II. To give some idea of how this procedure affects the results, Figs. 5 and 6 show a comparison of the DDCS's for a large angle for 100-keV, 300-keV, 1-MeV, and 4.2-MeV protons on Ar. A large angle was chosen in each case, to obviate any CEC effects.

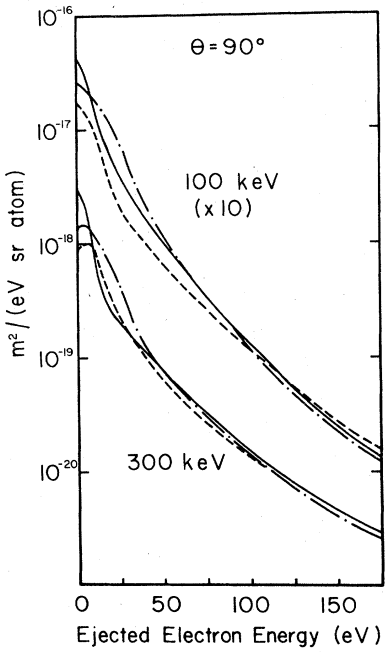

FIG. 5. DDCS for proton-impact ionization of argon as a function of the ejected electron energy at 90° angle of observation for the ejected electron. The theoretical curves are: solid line, HS calculation and dash-dot line, HF calculation. The dashed curves are the experimental data of Crooks and Rudd (Ref. 9).

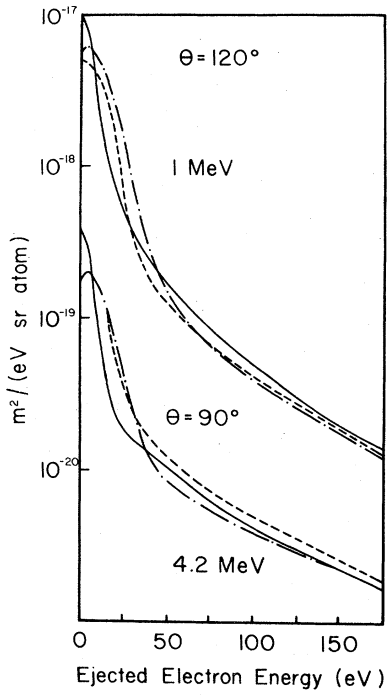

FIG. 6. Same as Fig. 5 except for higher proton energies. In the top curves, the angle of observation for the ejected electron is 120° and the experimental data are those of Criswell *et al.* (Ref. 13). In the bottom curves, the angle of observation is 90° and the experimental data are those of Gabler *et al.* (Ref. 10).

The first thing to note about the results is that above about 50 eV the two theoretical results are very similar. At lower energies, it is seen that the HS calculation is larger at threshold and drops down much faster than the HF result, indicative of a Cooper minimum at a lower energy.

Compared to the experiment, the HF result is closer than the HS right at threshold in all cases. At the lower proton energies, 100 and 300 keV, where the optical channel is not so dominant,[24] the HS does better than HF in the 10–50 eV region in absolute magnitude, while the HF does better on overall shape. At the higher proton energies, 1 and 4.2 MeV, the HF calculation is in better agreement with experiment than HS in both magnitude and shape. A substantially similar improvement will be obtained at all ejection angles, but due to the CEC process it will not be obvious at the forward angles for protons with energies around 100 keV or less. In any case, it is seen that the treatment of the $3p \rightarrow \epsilon d$ channel in HF does lead to improvements in the DDCS for ejection energies less than 50 eV, particularly right near the threshold. For energies greater than 50 eV, on the other hand, this comparison shows that HS wave functions are quite adequate.

It is interesting to note that the Cooper minimum in Ar, $3p \rightarrow \epsilon d$, is at a larger energy for HF than HS and that the experimental Cooper minimum lies between, but closer to HF.[21] Thus the HF improvement overcompensates in the position of the minimum. To get the Cooper minimum at just the right energy, correlation must also be included in addition to treating exchange exactly as the HF does. In particular, using a multiconfiguration ground state of the Ar atom, $(p)^6 + (p)^4(d)^2$, while keeping the rest of the calculation as HF, has been shown to place the Cooper minimum correctly.[25] Work on the DDCS employing this correlation effect is in progress.

V. SUBSHELL CONTRIBUTIONS

We now turn our attention to the contributions of the individual subshells to the cross sections summed over the various subshells for the HS calculation. At first glance, one might assume that the outer $3p$ subshell would give the major contribution to the sum. Generally, this expectation may be verified. However, some interesting exceptions are readily found if one examines the energy dependence of the various subshell contributions. Figure 7 presents the percent contributions of the various shells of argon to the sum over shells as a function of the energy of the ejected electron for various proton energies between 5 keV and 5 MeV. The result presented in Fig. 7 were all obtained for an ejected-electron angle of 0°. An examination of Fig. 7 reveals several interesting behaviors for the various shells. One of the striking features is the crossing of the $3s$ and $3p$ contributions for 5-keV protons. For electrons ejected with energies between 60–80 eV, the $3s$ shell contributes more strongly to the sum than the $3p$ shell. Outside of this narrow range, the $3p$ dominates as expected. This same type of structure can also be seen for 100-keV protons near an ejected-electron energy of 230 eV. The curves do not cross, however, and the $3s$ reaches a maximum contribution of 30%. This structure is not present for the higher proton energies for electron energies less than 300 eV.

For incident proton energies of 5 and 100 keV, the $n=2$ levels make a negligible contribution to the sum over shells. At the higher proton energies, the inner shells become more important, particularly for the higher ejected-electron energies. This phenomena can be understood as follows: the total ionization cross section for a subshell reaches a maximum approximately when the velocity of the incident particle matches the velocity of the electron in the subshell. This means that the $3p$ cross section will peak first, followed by the $3s$, $2p$, $2s$, and $1s$, respectively. The increased importance of the $2p$ and $2s$ shells at the higher proton energies reflects this peaking for the inner shells. It is interesting to note that for the higher proton energies, the $2p$ and $3s$ cross sections are comparable at the lower ejected-electron energies and that the $2p$ gives the dominant contribution to the sum over subshells for the higher ejected-electron energies. The $2s$ cross section, on the other hand, never becomes very significant for these parameters, contributing a maximum of around 10% and generally only a few percent or less. The K shell does not make a significant contribution to the sum over subshells for the proton and electron energies considered.

Figure 8 presents similar results for a large electron ejection angle of 120°. An examination of Fig. 8 reveals that the behavior of the various shells at 120° is qualitatively similar to that observed for 0°.

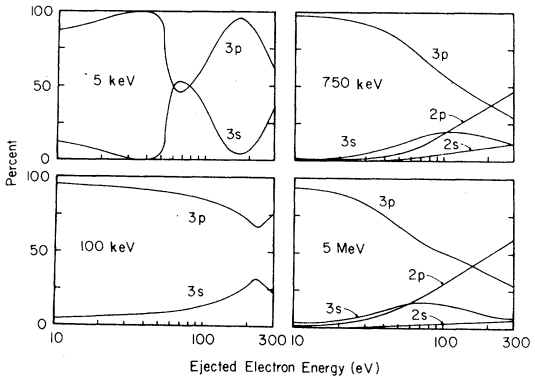

FIG. 7. Percent contribution of the various shells of argon to differential cross sections summed over shells as a function of the energy of the ejected electron. The results were all obtained from the HS calculation for a 0° observation angle for the ejected electron for proton energies between 5 keV and 5 MeV.

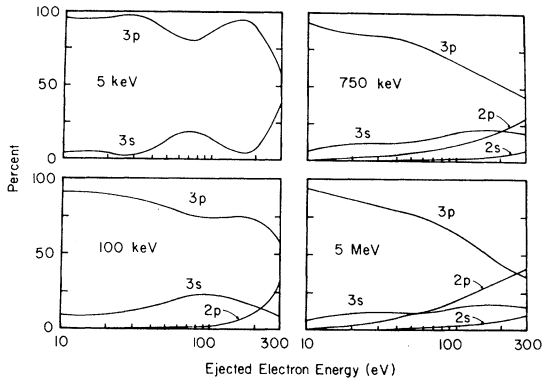

FIG. 8. Same as Fig. 7 except for an ejected-electron observation angle of 120°.

VI. K-SHELL CROSS SECTIONS

The present comparison between theory and experiment for differential cross sections summed over shells represents a more sensitive test of theory than single differential cross sections or total cross sections since much information can be lost in the integration process. However, an even more sensitive test of theory would lie in the examination of differential cross sections for individual subshells. At present, no experimental data exists for these cross sections and space limitations prohibit the display of the cross sections for all the subshells. However, over the last few years there has been an intense interest in K-shell ionization developed primarily by the expanded use of nuclear accelerators to do atomic physics. For this reason and the fact that the K-shell cross sections exhibit some interesting properties, we present differential cross sections for K-shell ionization in this section.

DDCS for ionization of the K shell of argon by 100-keV and 1-MeV proton impact are presented in Figs. 9 and 10, respectively, for a range of ejected electron energies between 10 and 300 eV. One of the first striking features noticeable from these figures is the fact that the cross section for backward ejection is larger than forward ejection. This feature becomes more prominant as the electron energy is lowered. The physical basis for this

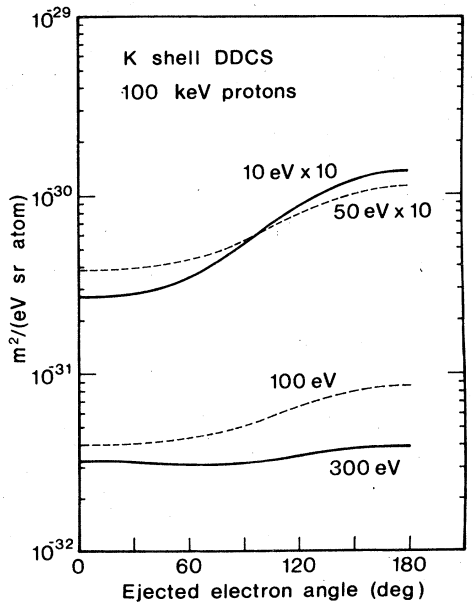

FIG. 9. DDCS for 100-keV proton-impact ionization of the K shell of argon as a function of the angle of observation for the ejected electron. The theoretical curves are HS calculations for ejected-electron energies between 10 and 300 eV.

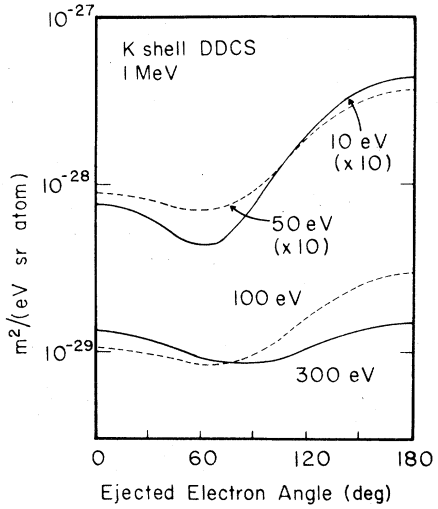

FIG. 10. Same as Fig. 9 except for 1-MeV incident protons.

increased flux in the backward direction can be understood using the following simplified model. Each electron in the atom is viewed as being trapped in a potential well and the well depth is equal to the ionization potential of the subshell for the electron. The incoming proton transfers energy to an electron creating a wave packet with enough energy to escape the well. The wave packet is formed inside the well with a preferentially forward direction. When the packet encounters the boundary of the well, it will be partially reflected—the amount of reflection being directly related to the ratio of the energy of the packet divided by the well depth. Significant reflection and subsequent ejection in the backward direction will occur only for small ratios of electron energies to ionization potentials. For ionization of the outer shells, this enhancement in the backward direction occurs at very low energies, due to the small binding energies, where other processes not included in a perturbation type calculation such as this could become important.

The situation is very different for ionization of a K shell, however. The ionization potential of the K shell of argon is 3.2 keV. Consequently, relatively high-energy electrons can represent a small fraction of this ionization potential and be strongly reflected, as seen in Figs. 9 and 10. The intriguing aspect of this phenomena associated with K-shell ionization lies in the fact that these ejected electrons have energies large enough that perturbation theory would be expected to be valid. As a result, this phenomena should be observable for K-shell ionization, whereas it may be obscured by other effects for the outer shells.

Another interesting feature of the differential K-shell cross section for a fixed proton energy is the weak dependence on the ejected-electron energy. If the factors of 10 were removed from the upper curves, all four of the angular distributions would lie on top of one another. Again, this phenomena can be understood in terms of the magnitude of the ejected-electron energies relative to the ionization potential of the shell. For the extreme outer shells, the ionization potentials lie in the energy region of 12–25 eV. An ejected-electron energy range of 12–300 eV represents a significant change relative to the ionization potentials of the outer shells but not of the inner shells. As a result, cross sections for the outer shells change more rapidly for this range of ejected-electron energies than those for the inner shells.

VII. CONCLUSION

We have calculated doubly differential cross sections for proton-impact ionization of argon within the framework of the Born approximation. Two different theoretical calculations were performed. In the first calculation, both the bound and continuum (ejected) electron wave function were calculated in the Hartree-Slater approximation. In the second calculation, the bound $3p$ and continuum ϵd wave functions were calculated in the Hartree-Fock approximation, while the remaining wave functions were calculated in the HS approximation. Comparison of these two calculations revealed that they were very similar for ejected-electron energies greater than about 50 eV for all the proton energies considered here. Fairly large differences between the calculations were observed for the lower electron energies. Neither the HS or HF calculations could be said to be in good agreement with all the experimental data at low electron energies. Overall, the HF calculation was in better agreement with the data than the HS calculation. The HF calculation did predict the threshold behavior much better than the HS calculation. It appears that correlated atomic wave functions will have to be used in the calculation before good agreement with the low ejected-electron energy data will be achieved. For electrons ejected with energy greater than 50 eV, the HS (or HF) calculation was, overall, in fairly good agreement with the experimental data. The only major discrepancies between the theory and experiment were seen at small angles when both the electron and proton were leaving the collision with comparable velocities. This disagreement is expected since this is the regime where charge exchange to the continuum is expected to be important and this effect has not been included in the calculations.

The contribution of the various subshells to the differential cross section summed over subshells was also examined. This study revealed that, as expected, the $3p$ contribution generally dominated the sum. However, the $3s$ and $2p$ subshells can represent major contributions to the sum. The relative weights of these two shells generally increase with increasing ejected-electron energy and, for the proper kinematical parameters, either the $3s$ or $2p$ can represent the major contributor to the sum. While the K-shell cross section never makes a significant contribution to the sum over shells, it does exhibit some interesting properties. One of the most interesting is that the cross section for backward ejection exceeds the cross section for forward ejection.

One of the primary results of this work is the demonstration that the Born approximation using realistic wave functions for the ejection electron can give theoretical DDCS for complex atoms that are essentially as reliable as those given for helium. This indicates that the Born approximation can be used to predict detailed differential cross sections for other ionization processes and other atoms as long as the angular dependence of the proton is not examined. Recently however, experiments are starting to be performed which examine the angular dependence of the protons.[26] Cross sections differential in the proton scattering angle for medium to large angles will probably require a distorted-wave type of approach.[27]

ACKNOWLEDGMENTS

One of the authors (D.H.M.) would like to acknowledge programming assistance by R. Lang and K. MacCollough. The work of one of us (D.H.M.) was supported by the Research Corporation, that of the other (S.T.M.) was supported by the U. S. Army Research Office.

[1] *Atomic Inner Shell Processes*, edited by B. Crasemann (Academic, New York, 1975) and references therein.

[2] *Proceedings of the International Conference on Inner Shell Ionization Phenomena and Future Applications*, edited by R. W. Fink, S. T. Manson, J. M. Palms, and P. V. Rao (AEC, Oak Ridge, Tennessee, 1973).

[3] M. E. Rudd, C. A. Sautter, and C. L. Bailey, Phys. Rev. 151, 20 (1966).

[4] N. Stolterfoht, Z. Phys. 248, 81 (1971).

[5]D. H. Madison, Phys. Rev. A 8, 2449 (1973).
[6]S. T. Manson, L. H. Toburen, D. H. Madison, and N. Stolterfoht, Phys. Rev. A 12, 60 (1975).
[7]M. E. Rudd and D. H. Madison, Phys. Rev. A 14, 128 (1976).
[8]J. Macek, Phys. Rev. A 1, 235 (1970).
[9]J. B. Crooks and M. E. Rudd, Phys. Rev. A 3, 1628 (1971).
[10]H. Gabler, U. Leithauser, and N. Stolterfoht (private communication).
[11]S. T. Manson and L. H. Toburen, in *The Physics of Electronic and Atomic Collisions*, edited by J. S. Risley and R. Geballe (University of Washington, Seattle, 1975), p. 751.
[12]M. E. Rudd, Radiat. Res. 64, 153 (1975).
[13]T. L. Criswell, L. H. Toburen, and M. E. Rudd, Phys. Rev. A 16, 508 (1977).
[14]D. J. Kennedy and S. T. Manson, Phys. Rev. A 5, 227 (1972).
[15]S. T. Manson, Adv. Electron. Electron Phys. 41, 73 (1976); 44, 1 (1977).
[16]F. Herman and S. Skillman, *Atomic Structure Calculations* (Prentice-Hall, Englewood Cliffs, 1963).
[17]A. R. P. Rau and U. Fano, Phys. Rev. 167, 7 (1968).
[18]J. W. Cooper, Phys. Rev. Lett. 128, 162 (1962).
[19]S. T. Manson and J. W. Cooper, Phys. Rev. A 165, 126 (1968).
[20]D. J. Kennedy and S. T. Manson, Phys. Rev. A 5, 227 (1972).
[21]L. H. Toburen and S. T. Manson, Chem. Phys. Lett. 30, 114 (1975).
[22]Y. K. Kim, Radiat. Res. 61, 21 (1975).
[23]Y. K. Kim, Radiat. Res. 64, 205 (1975).
[24]L. H. Toburen, S. T. Manson, and Y. K. Kim, Phys. Rev. A 17, 148 (1978).
[25]J. R. Swanson and L. Armstrong, Jr., Phys. Rev. A 15, 661 (1977).
[26]J. T. Park, J. M. George, J. L. Peacher, and J. E. Aldag, Phys. Rev. A 18, 48 (1978).
[27]D. H. Madison, R. V. Calhoun, and W. N. Shelton, Phys. Rev. A 16, 522 (1977).